Electronic Supplementary Material

Supplemental Methods

Categorization of study subjects. Social group affiliation was determined from direct observation of the study subjects and monthly censuses. We also confirmed social group affiliation by applying a community detection algorithm to raw social contact data [1]. For habituated individuals, sex was known from direct observation during annual captures. We assigned individuals to the following age classes: juveniles (1-2 years), subadults (3-4 years), adults (≥ 5 years); infants (< 1 year) were not included in the study. Sifaka exhibit formalized submissive signals, "chatter" vocalizations [2], which were used to assign intrasexual dominance rank among adult individuals in multi-male and/or multi-female groups. Among males in multi-male groups, one adult assumes the dominant position and is identifiable by a greasy, stained patch around his sternal scent gland [3]. In one-male groups, the resident male also exhibits this sternal staining. We used presence or absence of chest staining during censuses and captures to confirm relative male dominance (*i.e.*, dominant or subordinate, respectively) in multi-male groups. We determined group transfers using monthly census data.

Genetic sample collection and analyses. Ear tissue biopsies were collected from 72 individuals from five social groups between 2007 and 2012. Animals were captured using a blowpipe or CO_2 powered rifle to deliver 3/8 inch darts loaded with Telazol™ at a dosage of 25 mg per kg following the protocol of Lewis (2009) [4]. Tissue biopsies were stored in 70-90% ethanol for DNA preservation and kept at ambient temperature until their arrival at The University of Texas at Austin. Detailed information on DNA extraction, genotyping, and parentage protocols is provided in [5] and [6]. Briefly, each individual was genotyped for 14 variable microsatellite loci known to be variable in other populations of sifaka [7,8]. We used KINGROUP2 [9] to estimate the likelihood of pedigree relationships (cousin, half-sibling, full-sibling, and parent-offspring) among dyads. KINGROUP2 calculates the maximum likelihood ratios between a hypothesized pedigree relationship and a null hypothesis of no relationship. We considered particular dyads to be 'related' when likelihood ratios were significant ($P < 0.05$ based on 100,000 permutations) for any of the four primary hypotheses of first-order relatives versus the null hypothesis of 'unrelated.' All other dyads were considered to be unrelated. Based on these results, we constructed a 1-0 matrix of pairwise relatedness among 35 individuals, in which dyads were scored as either 'related' or 'unrelated.' Additionally, maternity and paternity were assessed for 32 offspring born in five social groups between 2007 and 2012 [5] using the maximum likelihood method implemented in CERVUS 3.0 [10]. We used these parentage results, in combination with highly significant relationships ($P < 0.001$) obtained using KINGROUP2, to construct a more finely-resolved relatedness matrix in which dyads were scored by their pedigree relationship (0.5, 0.25, 0.125, or 0).

Microbial diversity and composition among social groups. All statistical analyses were conducted using the statistical computing software R version 3.2.4 [11]. Figures were created using the *ggplot2* and *cowplot* packages [12,13].

Gut microbial richness: To test for differences in within-sample richness, diversity, and evenness among individuals, we generated 100 OTU tables rarefied to 39,532 reads (the smallest library size in the dataset) for each individual. After rarefaction, individual samples contained 651 to 3,599 unique OTUs ($\bar{x}$ = 2,482 $\pm$ 774 s.d. phylotypes per sample). We calculated mean rarefied richness (number of observed OTUs), Chao1 species richness, and Shannon's diversity index for each host using the rarefied OTU tables. Kruskal-Wallis tests adjusted for multiple comparisons (Benjamini-Hochberg approach) (*agricolae* package) [14] were used to evaluate whether bacterial richness and evenness per individual differed across social groups.

Microbiome sample clustering: All multivariate and community analyses were conducted using the *vegan* and *phyloseq* packages [15,16]. We quantified among-individual variation in gut microbial community composition by calculating Bray-Curtis dissimilarities and weighted Unifrac distances between samples. Permutational multivariate analysis of variance (PERMANOVA) [17] was carried out to assess differences in composition according to social group affiliation, age, sex, and sex/dominance rank (999 permutations). Clustering of taxonomic profiles was performed via partitioning of data around medoids (PAM clustering) using the *cluster* and *fpc* packages [18]. We maximized the silhouette index to assess the optimal number of clusters and the quality of the resulting clusters.

Differentially enriched microbial taxa: To identify socially structured bacterial phyla, families, and genera, we assessed differential abundance among social groups using the nonparametric SAMseq approach (*samr* package) [19]. This method uses repeated permutations for assessment of the false discovery rate (FDR). We limited analyses to bacterial phyla that occurred at least 50 times, families that occurred at least 100 times, and classifiable genera that occurred at least 100 times in the dataset. SAMseq analyses were performed separately for each taxonomic level using 1,000 permutations and 100 re-samplings. Differential abundance was considered significant if the FDR-adjusted P value was < 0.05.

Genetic relatedness and vertical inheritance. Because individuals within the same social group tend to be related (Mantel, r = 0.66, $P < 0.001$), we considered the confounding effect of kinship when testing for the effect of group membership on microbial communities. We used partial Mantel tests with 1,000 permutations, in which pairwise Bray-Curtis dissimilarity between samples was the dependent variable, group membership (scored as 0 for group members and 1 for individuals of different groups) or relatedness (scored as 0 for related and 1 for unrelated dyads) was the fixed effect, and relatedness or group membership respectively was a covariate. To evaluate vertical inheritance of gut microbial communities, we used a Kruskal-Wallis test (*coin* package) [20] with Monte Carlo sampling (10,000 permutations) to compare the mean pairwise Bray-Curtis dissimilarity among samples collected from related group members of the same maternal line (*i.e.*, mother-offspring, full sibling, and maternal half-sibling dyads), samples collected from related group members of different maternal lines (*i.e.*, father-offspring and paternal half-sibling dyads), and samples collected from unrelated group members. This analysis considered six maternal lines among Groups I-VI, respectively.

Dietary differences within and among social groups. To assess differences in diet among four social groups (II, III, IV, and V), we used direct observations of the plant parts consumed by 16 focal individuals during the six months preceding fecal sample collection (5 January 2012 to 19 June 2012; 365 focal hours). During these continuous focal animal follows lasting an average of six hours per day, all plant parts and plant species consumed, as well as the duration of feeding bouts, were recorded. Plant parts were divided into seven categories: (1) mature leaves, including those from *Diospyros latispatula, Bauhinia porosa, D. perrieri, Dalbergia greveana, Albizia androyensis, A. perrerii, Chadsia grevei, A. gummifera, Baudouinia fluggeiformis,* and *Colvillea racemosa*, (2) young leaves, including those from *A. androyensis, D. latispatula, A. perrerii, C. grevei, Chlorophytum falcatum, Terminalia fatrea,* and *Pourpartia* sp., (3) fruit, including those from *D. perrieri* and *Pourpartia sylvatica* (4) seeds, including those from *Diospyros* sp. and *Salacia madagascariensis* (5), bark from *Commiphora* sp., (6) stems, (7) flowers, including those from *A. androyensis, Noronhia alleizettei, Dalbergia clorocarpa*, and *Terminalia fatrea*. To quantify diet composition for each individual, we calculated the relative proportion of each plant part or plant species as the ratio of time spent feeding on that particular plant part or plant species to the total time spent feeding across all focal observations. We used Kruskal-Wallis tests with Monte Carlo resampling (10,000 permutations) to determine differences among social groups for the proportions of plant parts and plant species consumed. To assess whether microbiomes clustered according to diet, we computed pairwise Bray-Curtis dietary distances based on the relative proportion of time each animal was observed consuming plant species or plant parts. We used Mantel tests (1,000 permutations) to assess whether dietary profiles predicted microbial similarity among individuals.

Social interactions and gut microbiome composition. Social networks use *nodes* to represent individuals, or groups of individuals, and *edges* to connect nodes based on empirical proximity, social interactions, or shared space. To test whether physical contact predicts similarity in gut microbiome composition for sifaka, we constructed a social network based on socio-affiliative interactions observed during the year preceding and including fecal sample collection (5 September 2011 to 28 July 2012; 6,972 total interactions). Behavioral data were collected for four social groups (II, III, IV, V) on a rotating schedule such that each social group was generally observed for three consecutive days twice per month. All occurrences of non-aggressive body contacts, proximity within 1m, and allogrooming were collected on 22 adult and subadult individuals during one-hour focal animal samples [21]. Observations of social behavior were recorded continuously, based upon a previously published ethogram for this species [22]. On average, each focal animal was followed for 38.8 ($\pm$ 15.1) h, comprising a total of 854.3 focal hours. Juveniles were not observed as focal individuals, but were included in our analysis if they were observed interacting with adult or subadult focal individuals. Thus, the socio-affiliative behavior-based network comprised 33 individuals total. In addition to the continuous recording of focal animal behavior, the location and distance to the focal animal of all group members (including juveniles) were recorded every 10 min via scan sampling [21].

We calculated grooming indices using the proportion of time two individuals spent grooming each other, while controlling for the time individuals were observed as focal animals [23]. We defined the grooming index as:

$$Groom_{AB} = \frac{\sum(A + B)}{\sum A + \sum B} \quad (1)$$

wherein A is the time individual A was observed as a focal animal, B is the time individual B was observed as a focal animal, and A + B is the time A and B were observed grooming. Network edges were thus weighted according to grooming indices, such that pairs with higher indices had thicker edges. We used edge density (the ratio of the number of edges and the number of possible edges) to describe social connectivity within social groups. We used a Pearson correlation test to examine the influence of edge density on Bray-Curtis dissimilarities and weighted Unifrac distances among group members. To quantify the extent of community structure in the social network, we calculated network modularity (Q) using the edge betweenness community detection algorithm [1]. This algorithm partitions the network into "modules" that are densely connected themselves and sparsely connected to other modules. The modularity score Q ranges from zero for randomly connected networks to greater than 0.3 for networks with substantial community structure [1]. To measure how direct and indirect contacts potentially influence gut microbial composition, we calculated inverse weighted path lengths [24]:

$$E_{ij} = \min \sum_{i,j} \frac{1}{w_{ij}} \quad (2)$$

where E_{ij} is the smallest sum of the inverse weights of edges or 'social distance' between each pair of individuals. By incorporating indirect contacts into our social network analysis, we were able to quantify social relationships between individuals that were not necessarily observed as focal individuals (*e.g.*, juveniles). To assess whether sociability affects bacterial species richness within individual microbiomes, we calculated each animal's weighted degree centrality (*i.e.*, the sum of its edge weights) in the grooming network. We also calculated separate outward and inward weighted degree centralities corresponding to the duration of grooming initiated or received by each individual in the grooming network. We constructed social networks and calculated network statistics using the *igraph* package [25].

Predictors of similarity in microbiome taxonomic composition: We used mixed-effect regression models to fit the Bray-Curtis dissimilarity and weighted Unifrac distance data to potential social and genetic predictors of pairwise similarity in microbiome composition. The variables included in model selection were group membership ('same' versus 'different'), grooming network path length (*i.e.*, social distance) between individuals, and genetic relatedness ('related' versus 'unrelated'). An individual could appear interchangeably as individual A or individual B in pairwise associations; thus, we controlled for autocorrelation by modeling the identities of animals in each pair as random effects. Model components were compared using

Deviance Information criterion (DIC). Lower values indicate a better fit of the model to the data, and a difference of 5 units is the customary threshold for distinguishing between models. We adopted a Bayesian approach using the *MCMCglmm* package [26] and fit our models via Markov chain Monte Carlo (MCMC). We ran two sets of models to explain Bray-Curtis dissimilarities and weighted Unifrac distances, respectively, for 167 pairs of sifaka among the four social groups (II, III, IV, V) for which behavioral data were available. For each model, the MCMC chain was run for 300,000 iterations, with 25,000 iterations for burn in and a thinning interval of 15. We observed minimal autocorrelation between recorded iterations, and traces of the sampled output indicated that the models converged. Because Bray-Curtis dissimilarity and weighted Unifrac values are continuous proportions, we also fit mixed-effect Beta regression models to the microbial dissimilarity data using the *glmmADMB* package [26] and obtained results analogous to those from the *MCMCglmm* package.

To evaluate the potential confounding effect of spatial proximity, we constructed additional social networks based on proximities within 1m observed during the year (13,340 total interactions among 34 individuals) and six months (7,482 interactions among 29 individuals) prior to and including fecal sample collection. For each time period, we used a partial Mantel test (1,000 permutations) to assess whether the correlation between the grooming network and microbiome dissimilarity matrix was driven by spatial proximity (represented using a matrix of pairwise proximity path lengths). To assess whether close grooming partners consumed more similar diets, we computed Bray-Curtis dietary distances among individuals (N = 16) based on the relative proportions of time individuals were observed consuming plant species or plant parts. We then constructed a social network based on the grooming interactions observed among only these individuals. Partial Mantel tests (1,000 permutations) assessed whether the correlation between social distance and microbiome dissimilarity was driven by similarity in plant parts or plant species consumed. Pairwise Bray-Curtis dissimilarity between samples was the dependent variable, six-month grooming path length (the same time period as feeding data collection) between individuals was the fixed effect, and pairwise Bray-Curtis dietary distance was a covariate.

Predictors of within-host microbial diversity: We applied a mixed model approach to determine predictors of within-host bacterial species richness for 29 individuals. Poisson GLMMs were fit to the data via maximum likelihood (link="log", nAGQ = 100, *lme4* package) [27]. We considered bacterial species richness to be the mean number of unique OTUs for each host calculated from 100 OTU tables rarefied to 38,663 reads. Because sifaka social groups had inherently different levels of microbial richness (Fig. S3), social group affiliation was included as a random effect. Our fixed-effect variables included host sociability (*i.e.*, weighted degree centrality in the grooming network), age (adult, subadult, or juvenile), scent-marking rate (mean number of scent-marks per hour), and dietary diversity (Shannon's diversity index based on the proportion of time observed foraging on plant parts or plant species). We tested age and host sociability together in the first model. We then separately tested the influence of network centrality in only adult individuals to avoid the confounding effect of age. In the second model, we tested whether OTU richness was specifically associated with initiating or receiving

grooming by including outward weighted degree centrality or inward weighted degree centrality as covariates. Because we had scent-marking data for only 19 individuals, scent-marking rate was tested separately from the other covariates in a third model. In the fourth model, we tested whether dietary evenness of plant parts and plant species consumed influenced microbial richness among the 16 individuals for which dietary data were available.

Supplemental References

1. Newman, Girvan M. 2004 Finding and evaluating community structure in networks. *Phys. Rev. E* **69**, 26113. (doi:10.1103/PhysRevE.69.026113)
2. Kraus C, Heistermann M, Kappeler PM. 1999 Physiological suppression of sexual function of subordinate males: a subtle form of intrasexual competition among male sifakas (*Propithecus verreauxi*)? *Physiol. Behav.* **66**, 855–861. (doi:10.1016/S0031-9384(99)00024-4)
3. Lewis RJ, van Schaik CP. 2007 Bimorphism in male Verreaux's sifaka in the Kirindy Forest of Madagascar. *Int. J. Primatol.* **28**, 159–182. (doi:10.1007/s10764-006-9107-3)
4. Lewis RJ. 2009 Chest staining variation as a signal of testosterone levels in male Verreaux's Sifaka. *Physiol. Behav.* **96**, 586–92. (doi:10.1016/j.physbeh.2008.12.020)
5. Abondano LA. 2014 Male reproductive skew in multimale social groups of Verreaux's sifaka (*Propithecus verreauxi*) at Kirindy Mitea National Park, Madagascar.
6. Van Belle S, Estrada A, Di Fiore A. 2014 Kin-biased spatial associations and social interactions in male and female black howler monkeys (*Alouatta pigra*). *Behaviour* **151**, 2029–2057. (doi:http://dx.doi.org/10.1163/1568539X-00003229)
7. Lawler RR, Richard a F, Riley M a. 2001 Characterization and screening of microsatellite loci in a wild lemur population (*Propithecus verreauxi verreauxi*). *Am. J. Primatol.* **55**, 253–9. (doi:10.1002/ajp.1058)
8. Rakotoarisoa G, Shore GE, Mcguire SM, Engberg SE, Edward E. Louis J, Brenneman R a. 2006 Characterization of 13 microsatellite marker loci in Verreaux's sifaka (*Propithecus verreauxi*). *Mol. Ecol. Notes* **6**, 1122–1125. (doi:10.1111/j.1471-8286.2006.01458.x)
9. Konovalov DA, Manning C, Henshaw MT. 2004 KINGROUP: A program for pedigree relationship reconstruction and kin group assignments using genetic markers. *Mol. Ecol. Notes* **4**, 779–782. (doi:10.1111/j.1471-8286.2004.00796.x)
10. Kalinowski ST, Taper ML, Marshall TC. 2007 Revising how the computer program CERVUS accommodates genotyping error increases success in paternity assignment. *Mol. Ecol.* **16**, 1099–1106. (doi:10.1111/j.1365-294X.2007.03089.x)
11. R Core Team. 2016 R: A language and environment for statistical computing.
12. Wickham H. 2009 *ggplot2: Elegant Graphics for Data Analysis*. New York, New York: Springer-Verlag.
13. Wilke CO. 2015 Cowplot: streamlined plot theme and plot annotations for ggplot2. *R Packag. version 0.5.0. Available https//cran.rproject.org/web/packages/cowplot/index.html*
14. de Mendiburu F. 2015 agricolae: Statistical Procedures for Agricultural Research.

15. McMurdie PJ, Holmes S. 2013 Phyloseq: An R Package for Reproducible Interactive Analysis and Graphics of Microbiome Census Data. *PLoS One* **8**. (doi:10.1371/journal.pone.0061217)

16. Oksanen J *et al.* 2016 vegan: Community Ecology Package.

17. Anderson MJ. 2001 A new method for non-parametric multivariate analysis of variance. *Austral Ecol.* **26**, 32–46. (doi:10.1111/j.1442-9993.2001.tb00081.x)

18. Maechler M, Rousseeuw P, Struyf A, Hubert M, Hornik K. 2012 Cluster: cluster analysis basics and extensions. *R Packag. version* **1**, 56.

19. Fernandes AD, Reid JN, Macklaim JM, McMurrough T a, Edgell DR, Gloor GB. 2014 Unifying the analysis of high-throughput sequencing datasets: characterizing RNA-seq, 16S rRNA gene sequencing and selective growth experiments by compositional data analysis. *Microbiome* **2**, 15. (doi:10.1186/2049-2618-2-15)

20. Hothorn T, Hornik K, van de Wiel M, Zeileis A. 2008 Implementing a class of permutation tests: The coin package. *J. Stat. Softw.* **28**, 1–23. (doi:10.18637/jss.v028.i08)

21. Altmann J. 1974 Observational study of behavior: sampling methods. *Behaviour* **49**, 227–267.

22. Brockman DK. 1994 Reproduction and mating system of Verreaux's sifaka, Propithecus vereauxi, at Beza Mahafaly, Madagascar. *Yale Univ.* (doi:10.16953/deusbed.74839)

23. Machanda ZP, Gilby IC, Wrangham RW. 2013 Male-Female Association Patterns Among Free-ranging Chimpanzees (*Pan troglodytes schweinfurthii*). *Int. J. Primatol.* **34**, 917–938. (doi:10.1007/s10764-013-9707-7)

24. Latora V, Marchiori M. 2003 Economic small-world behavior in weighted networks. *Eur. Phys. J. B* **32**, 249–263. (doi:10.1140/epjb/e2003-00095-5)

25. Csardi G, Nepusz T. 2006 The igraph software package for complex network research. *InterJournal* **Complex Sy**, 1695.

26. Skaug H, Fournier D, Nielsen A, Magnusson A, Bolker B. 2016 glmmADMB: Generalized Linear Mixed Models using 'AD Model Builder'.

27. Bates D, Mächler M, Bolker B, Walker S. 2015 Fitting Linear Mixed-Effects Models Using {lme4}. *J. Stat. Softw.* **67**, 1–48. (doi:10.18637/jss.v067.i01)

Supplemental Figures

Figure S1. Map indicating the location of Ankoatsifaka Research Station. Ankoatsifaka Research Station (20°47.69′S, 44°9.88′E) is located in a terrestrial section of Kirindy Mitea National Park, near the western coast of Madagascar.

Figure S2. Relative abundances of bacterial families among seven Verreaux's sifaka social groups inhabiting Kirindy Mitea National Park. The most prevalent families in the sifaka gut microbiome were Lachnospiraceae, Ruminococcaceae, Clostridiaceae, [Coprobacillaceae], Coriobacteriaceae, Streptococcaceae, Veillonellaceae, (Firmicutes), Enterobacteriaceae (Proteobacteria), Bacteroidaceae, Prevotellaceae, and [Paraprevotellaceae] (Bacteroidetes).

Figure S3. Mean phylotype observed richness, Chao1 species richness, and Shannon's diversity in seven Verreaux's sifaka social groups inhabiting Kirindy Mitea National Park. The three indices were calculated from 100 OTU tables rarefied to 39,532 reads for each sample. Differences among social groups were evaluated using Kruskal-Wallis tests adjusted for multiple comparisons (* $P < 0.05$).

Figure S4. Average silhouette width values for partitioning around medoids (PAM) clustering with different numbers of clusters (k). Two (clusters) was chosen as the optimal number. Analyses were based on Bray-Curtis dissimilarities (left) and weighted Unifrac distances (right) among 47 Verreaux's sifaka microbiome samples collected in Kirindy Mitea National Park.

Figure S5. Principal coordinates plot of Bray-Curtis dissimilarities showing ecological distances among 47 Verreaux's sifaka samples. Males that transferred social groups during the year prior to sample collection (diamonds) are labeled with the direction of immigration.

Figure S6. Within social groups, resident sifaka did not share more bacterial phylotypes than pairs of recent immigrants and residents. The difference in microbial distance among resident pairs versus immigrant-resident pairs were evaluated using a permutational Wilcoxon-Mann-Whitney test.

Figure S7. Several bacteria genera, including microorganisms considered to be opportunistic pathogens, were differentially abundant across seven social groups of Verreaux's sifaka in Kirindy Mitea National Park (FDR-adjusted $P < 0.05$).

Figure S8. Diet composition for the six months prior to fecal sample collection for 16 Verreaux's sifaka across four social groups (II, III, IV, V) in Kirindy Mitea National Park.

Figure S9. Differences among four Verreaux's sifaka social groups in the proportion of foraging time spent consuming various plant parts (mature leaves, flowers, fruit, bark, seeds, larvae, stems, young leaves). Differences among groups were evaluated using permutational Kruskal-Wallis tests adjusted for multiple comparisons (* $P < 0.05$).

Figure S10. Differences among four Verreaux's sifaka social groups in the proportion of foraging time spent consuming the most common food tree species within Kirindy Mitea National Park. Differences among groups were evaluated using permutational Kruskal-Wallis tests adjusted for multiple comparisons (** $P < 0.01$, * $P < 0.05$).

Figure S11. Inter-individual differences in dietary profiles among 16 Verreaux's sifaka in four social groups inhabiting Kirindy Mitea National Park. **A.** Principal coordinates plot of Bray-Curtis dissimilarities among sifaka plant part dietary profiles. Dietary profiles are based on the proportion of foraging time spent consuming various plant parts (mature leaves, flowers, fruit, bark, seeds, larvae, stems, young leaves). **B.** Principal coordinates plot of Bray-Curtis dissimilarities among sifaka plant species dietary profiles. Dietary profiles are based on the proportion of foraging time spent consuming the most common food tree species within Kirindy Mitea National Park.

Figure S12. Although adjacent social groups shared more bacterial phylotypes than non-adjacent social groups, groups maintained distinct gut microbiota despite overlapping home ranges. Differences among groups were evaluated using permutational Kruskal-Wallis tests adjusted for multiple comparisons (*** $P < 0.001$).

Figure S13. Social groups with higher edge densities have more homogeneous microbiome compositions. Within-social group edge density is the ratio of the number of edges and the number of possible edges. We used a Pearson correlation test to examine the influence of edge density on Bray-Curtis dissimilarities and weighted Unifrac distances among group members.

Fig S14. Vertical inheritance and genetic relatedness correlate with microbiome similarity between groups but not within groups. **A.** At the population level, related individuals have more similar microbial communities than unrelated individuals (permutational Kruskal-Wallis, FDR-adjusted $P < 0.01$). **B.** Within social groups, related individuals of the same or different maternal line do not necessarily share more bacterial phylotypes than unrelated group members (permutational Kruskal-Wallis, FDR-adjusted $P > 0.05$). Analyses were based on Bray-Curtis dissimilarities among 35 Verreaux's sifaka microbiome samples collected in Kirindy Mitea National Park.

Figure S15. Scent-marking rate predicts within-host gut microbiome richness for Verreaux's sifaka (N = 19 individuals) inhabiting Kirindy Mitea National Park. Although we differentiate individuals by sex and adult male chest status in the figure, we did not include chest status or sex as covariates in our predictive model of gut microbiome richness.

Figure S16. Map of Verreaux's sifaka social group home ranges during the study period (Groups I-VI). Group Camp is not included because it is an unmarked group for which we did not have demographic, census, or behavioral data.

Figure S1

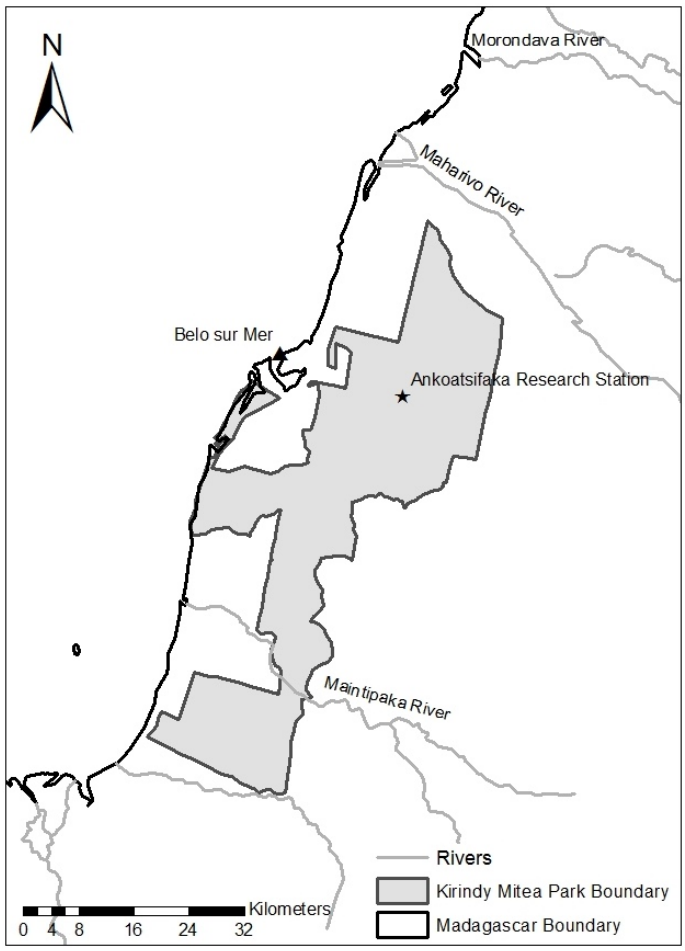
N
Morondava River
Maharivo River
Belo sur Mer
Ankoatsifaka Research Station
Maintipaka River
Rivers
Kirindy Mitea Park Boundary
Madagascar Boundary
Kilometers
0 4 8 16 24 32

Figure S2

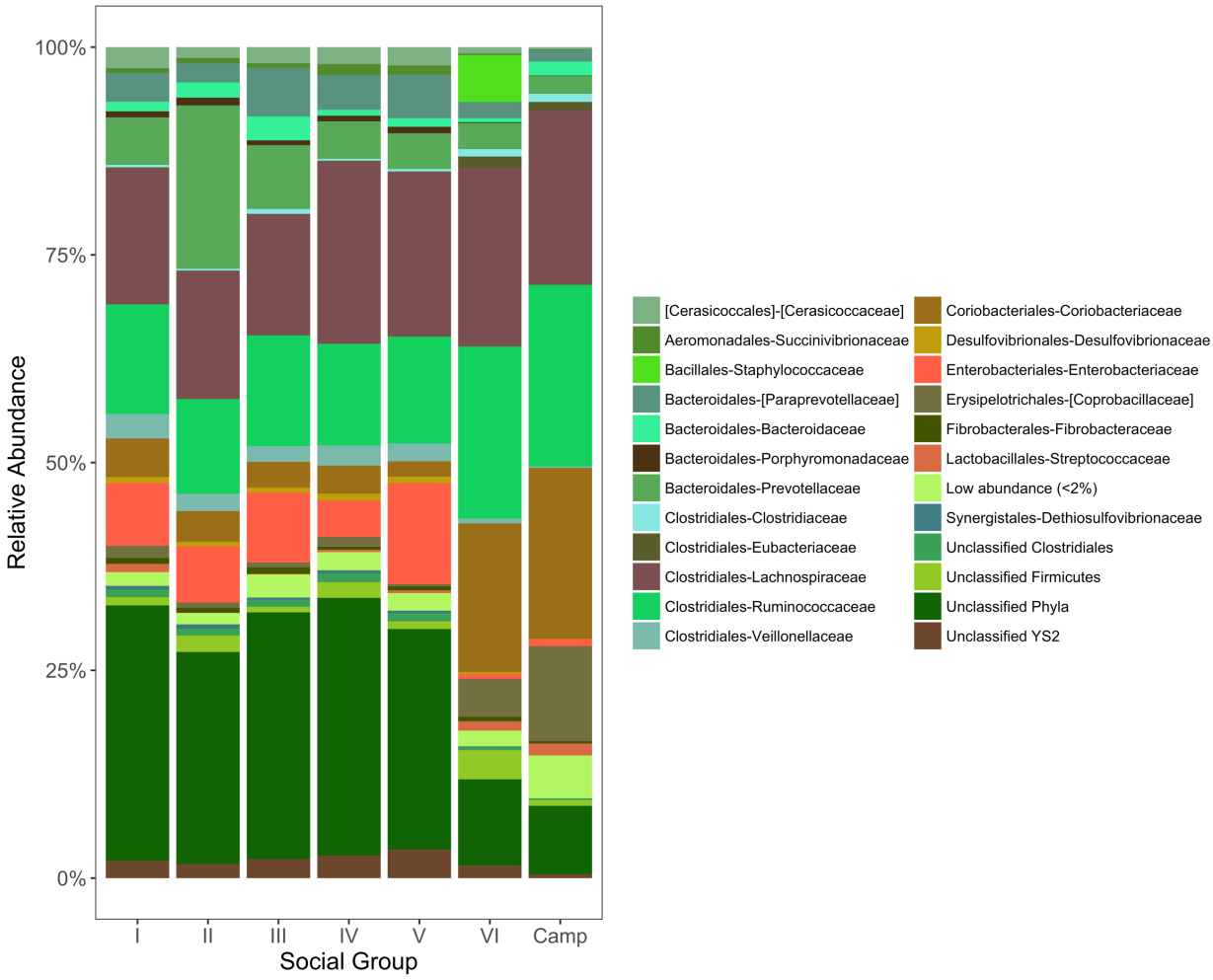
100%
75%
50%
25%
0%
Relative Abundance
I
II
III
IV
V
VI
Camp
Social Group
[Cerasicoccales]-[Cerasicoccaceae]
Aeromonadales-Succinivibrionaceae
Bacillales-Staphylococcaceae
Bacteroidales-[Paraprevotellaceae]
Bacteroidales-Bacteroidaceae
Bacteroidales-Porphyromonadaceae
Bacteroidales-Prevotellaceae
Clostridiales-Clostridiaceae
Clostridiales-Eubacteriaceae
Clostridiales-Lachnospiraceae
Clostridiales-Ruminococcaceae
Clostridiales-Veillonellaceae
Coriobacteriales-Coriobacteriaceae
Desulfovibrionales-Desulfovibrionaceae
Enterobacteriales-Enterobacteriaceae
Erysipelotrichales-[Coprobacillaceae]
Fibrobacterales-Fibrobacteraceae
Lactobacillales-Streptococcaceae
Low abundance (<2%)
Synergistales-Dethiosulfovibrionaceae
Unclassified Clostridiales
Unclassified Firmicutes
Unclassified Phyla
Unclassified YS2

Figure S3

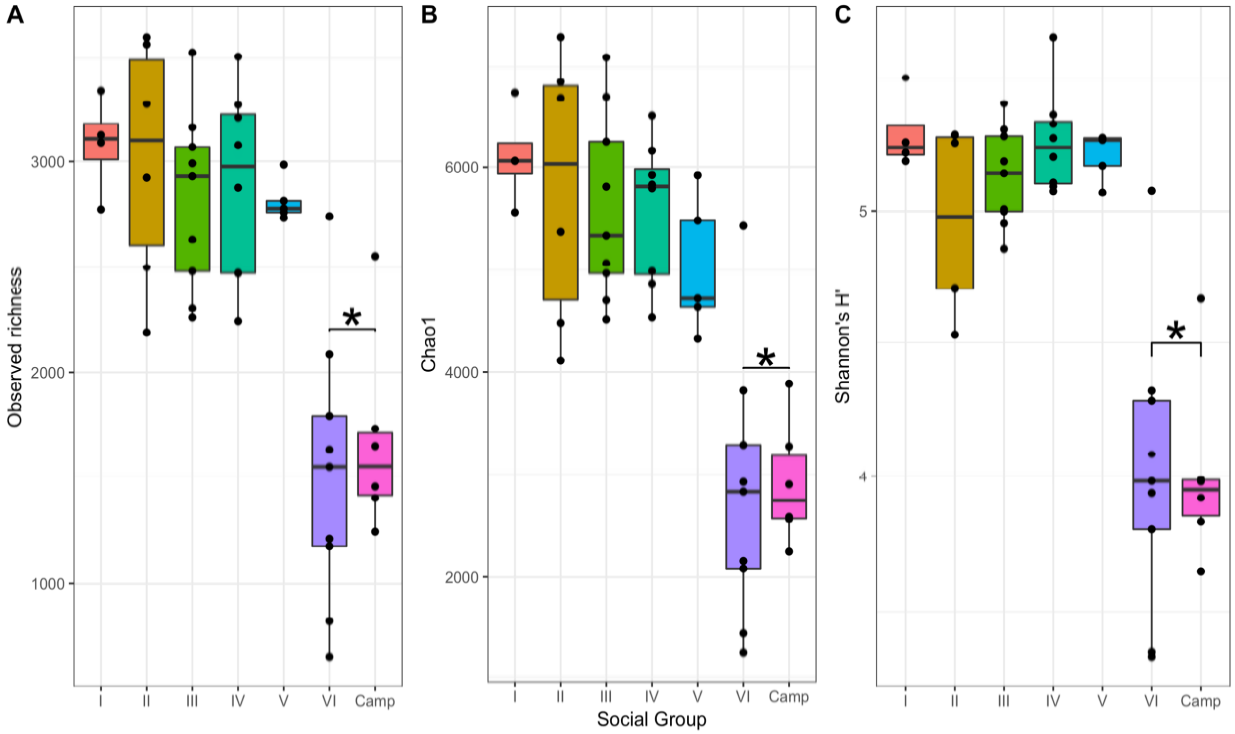
A
Observed richness
3000
2000
1000
I
II
III
IV
V
VI
Camp
*
B
Chao1
6000
4000
2000
Social Group
C
Shannon's H'
5
4

374 **Figure S4**

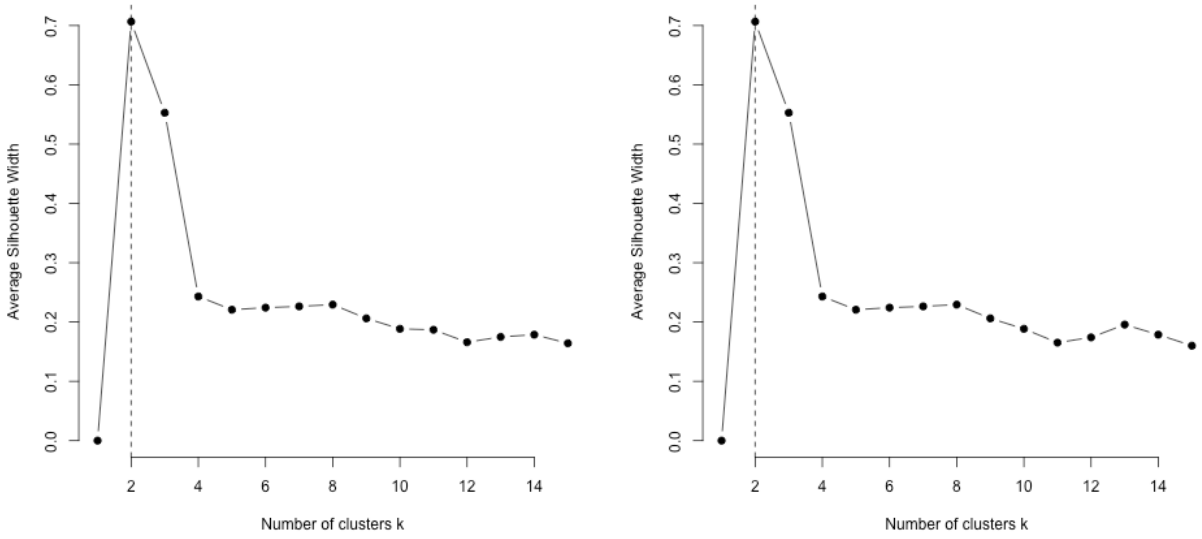

375
376

Figure S5

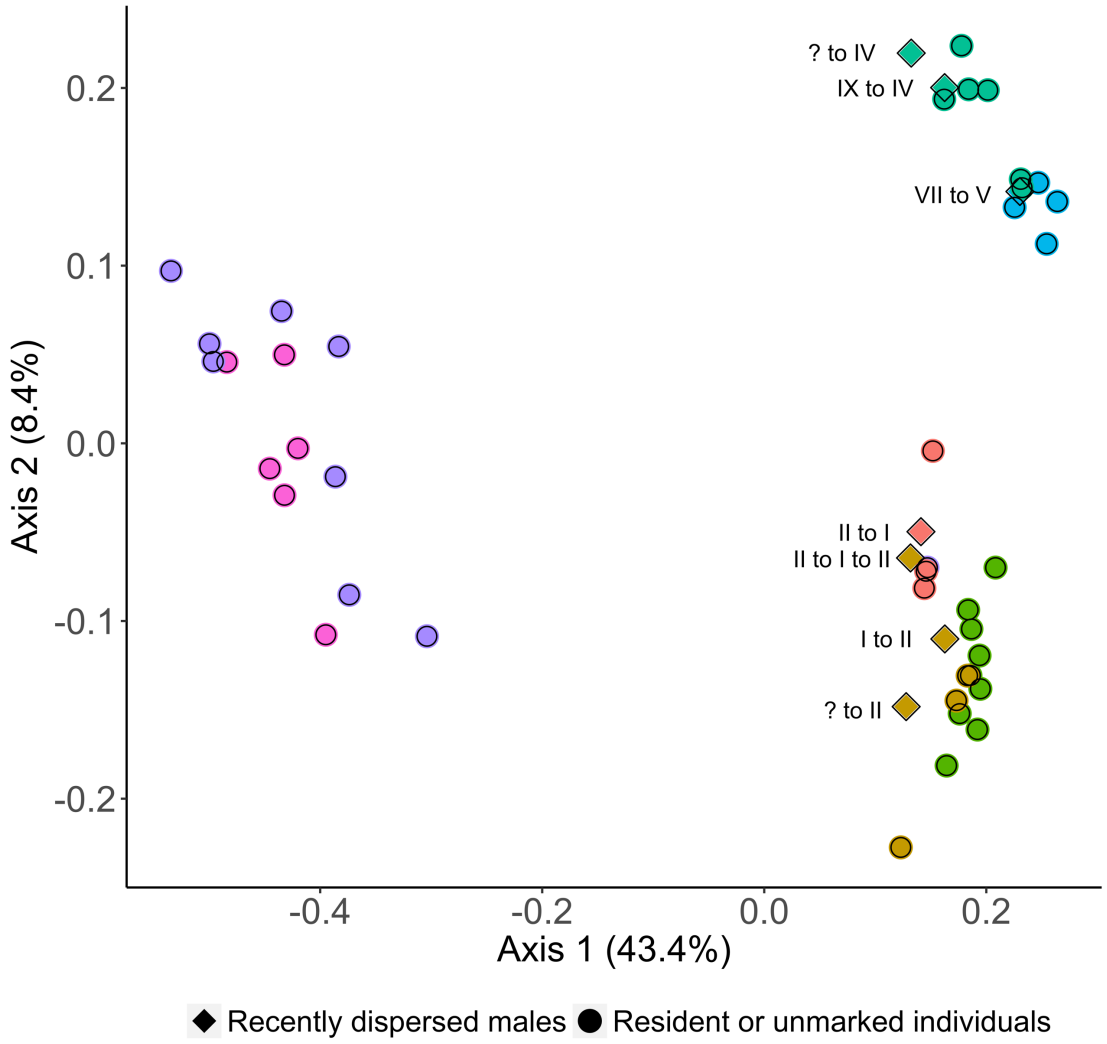

sic

Figure S6

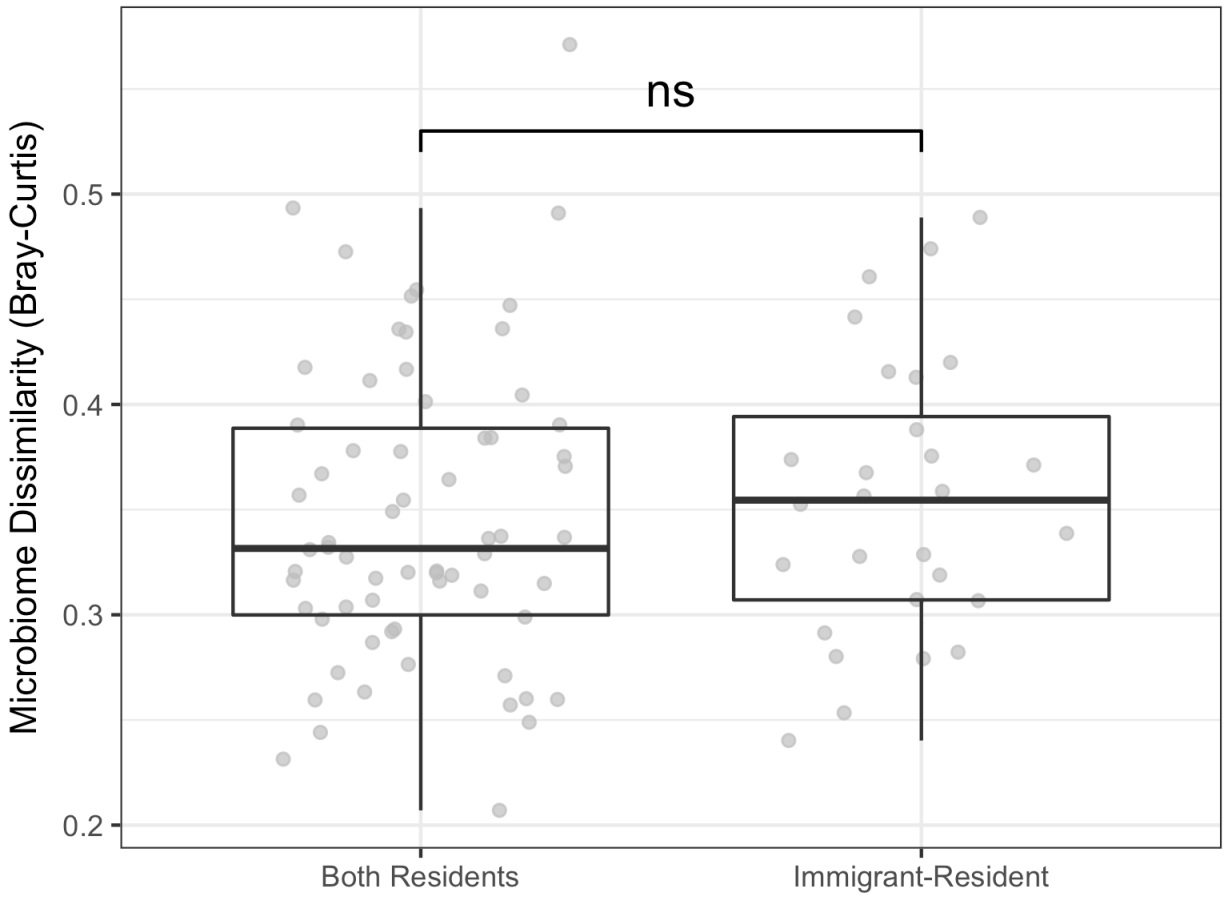
ns
Microbiome Dissimilarity (Bray-Curtis)
0.5
0.4
0.3
0.2
Both Residents
Immigrant-Resident

Figure S7

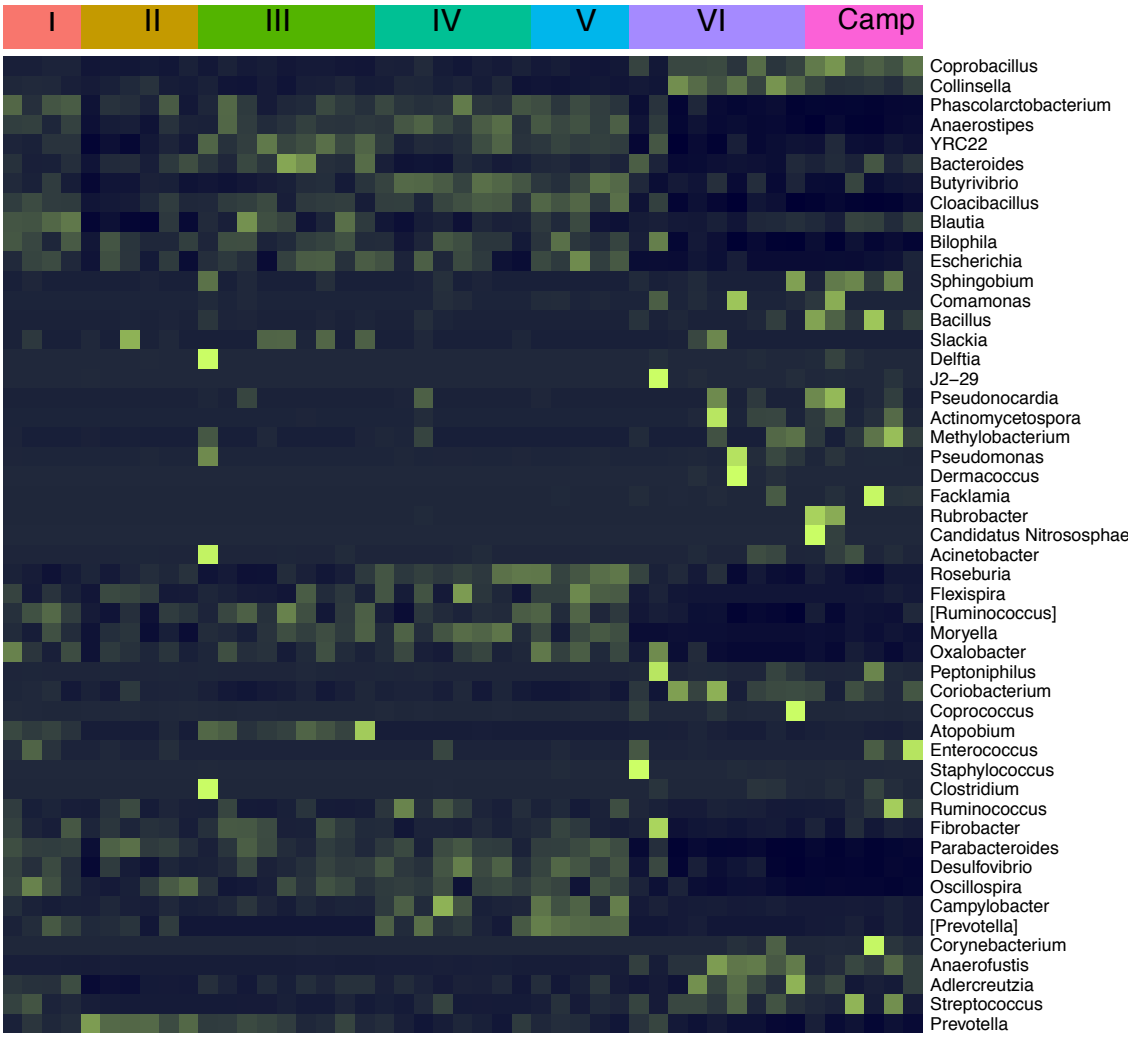
I
II
III
IV
V
VI
Camp
Coprobacillus
Collinsella
Phascolarctobacterium
Anaerostipes
YRC22
Bacteroides
Butyrivibrio
Cloacibacillus
Blautia
Bilophila
Escherichia
Sphingobium
Comamonas
Bacillus
Slackia
Delftia
J2−29
Pseudonocardia
Actinomycetospora
Methylobacterium
Pseudomonas
Dermacoccus
Facklamia
Rubrobacter
Candidatus Nitrososphae
Acinetobacter
Roseburia
Flexispira
[Ruminococcus]
Moryella
Oxalobacter
Peptoniphilus
Coriobacterium
Coprococcus
Atopobium
Enterococcus
Staphylococcus
Clostridium
Ruminococcus
Fibrobacter
Parabacteroides
Desulfovibrio
Oscillospira
Campylobacter
[Prevotella]
Corynebacterium
Anaerofustis
Adlercreutzia
Streptococcus
Prevotella

Figure S8

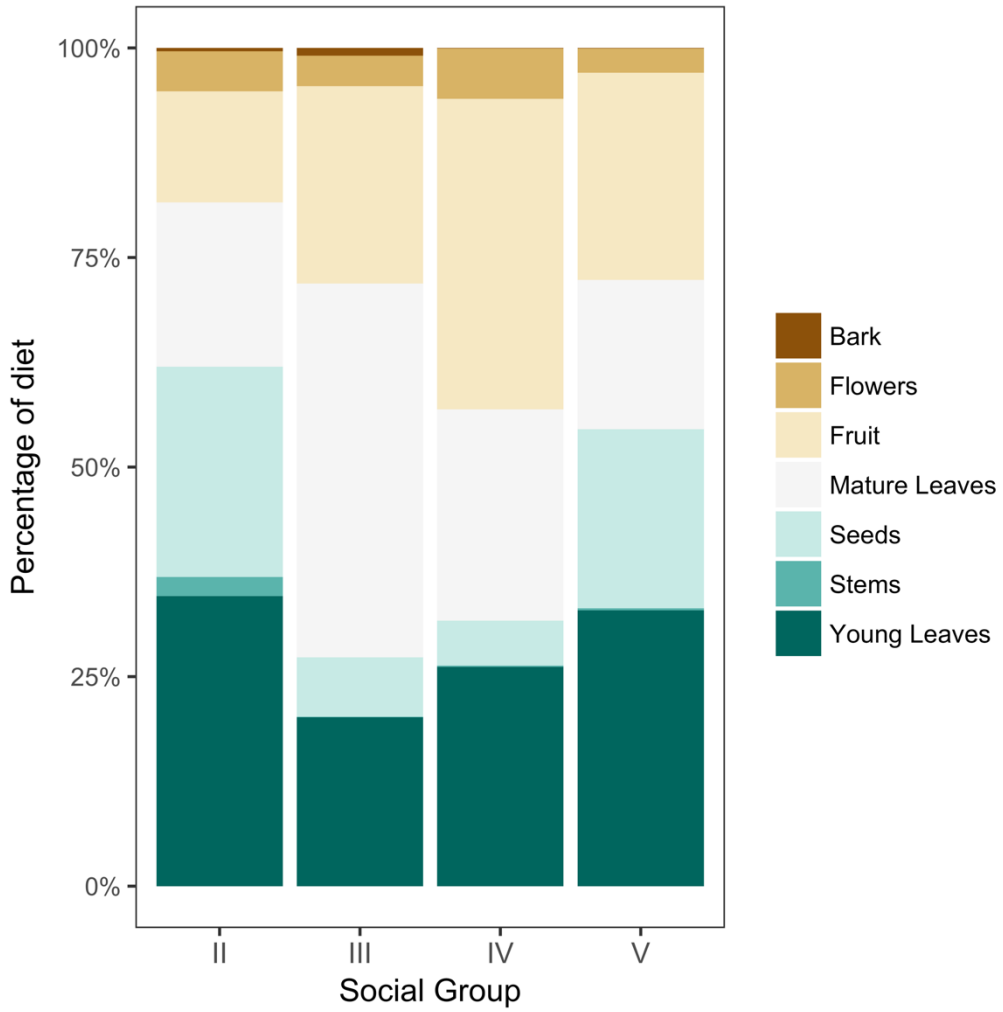
100%
75%
50%
25%
0%
Percentage of diet
II
III
IV
V
Social Group
Bark
Flowers
Fruit
Mature Leaves
Seeds
Stems
Young Leaves

Figure S9

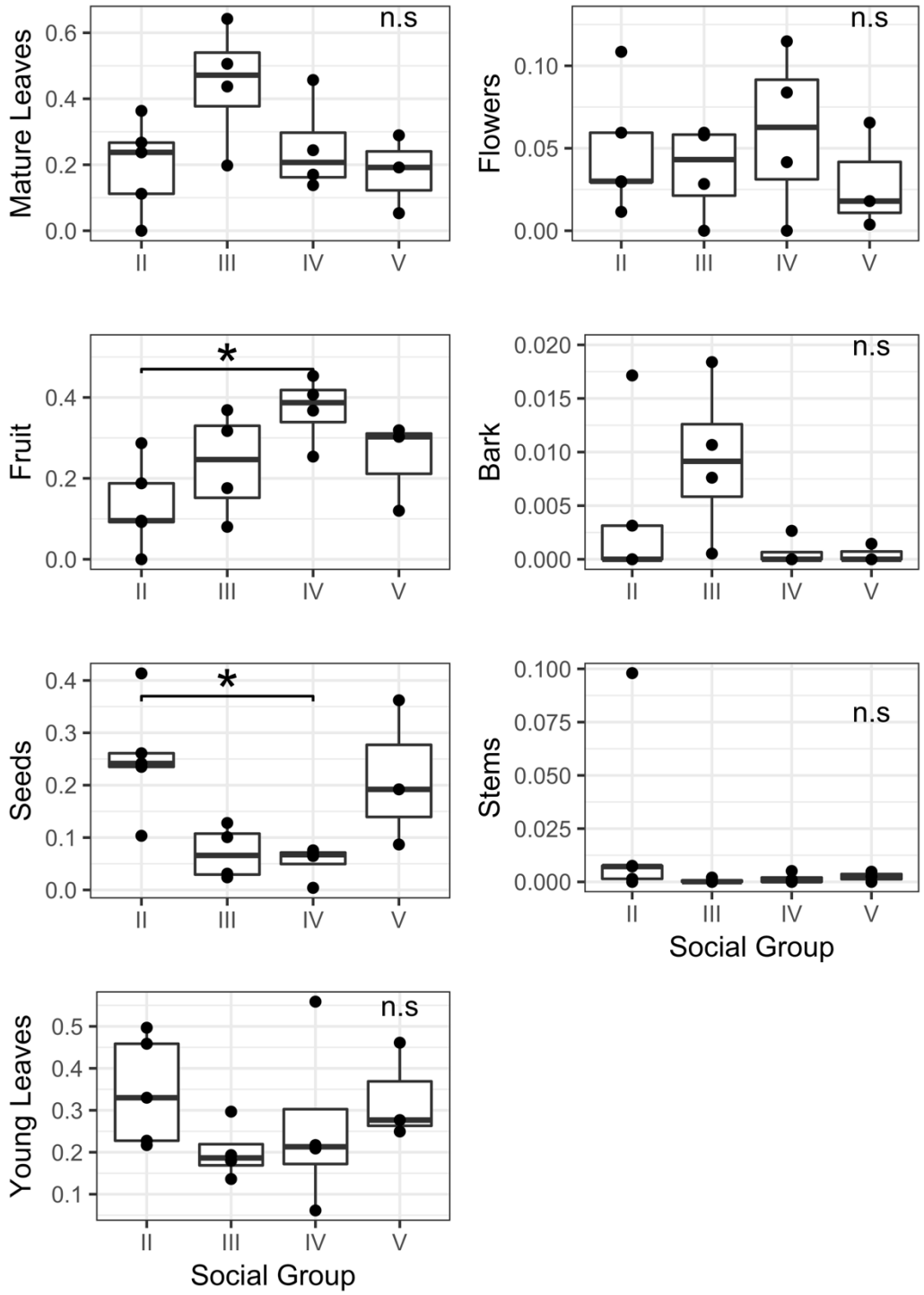
Mature Leaves
n.s
Flowers
n.s
Fruit
*
Bark
n.s
Seeds
*
Stems
n.s
Young Leaves
n.s
II
III
IV
V
Social Group

Figure S10

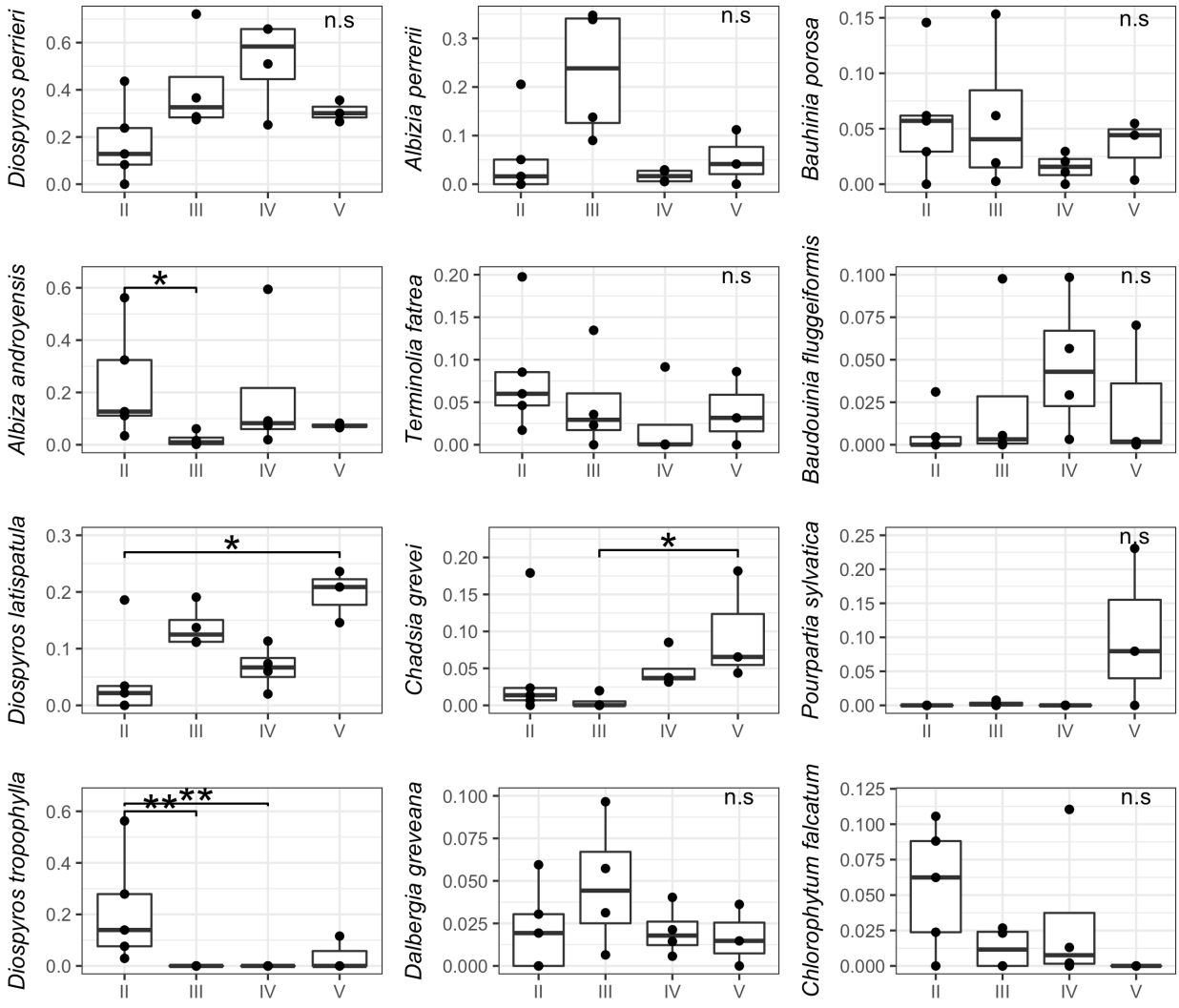
Diospyros perrieri
n.s
Albizia perrerii
n.s
Bauhinia porosa
n.s
Albiza androyensis
*
Terminolia fatrea
n.s
Baudouinia fluggeiformis
n.s
Diospyros latispatula
*
Chadsia grevei
*
Pourpartia sylvatica
n.s
Diospyros tropophylla
**
Dalbergia greveana
n.s
Chlorophytum falcatum
n.s
II
III
IV
V

Figure S11

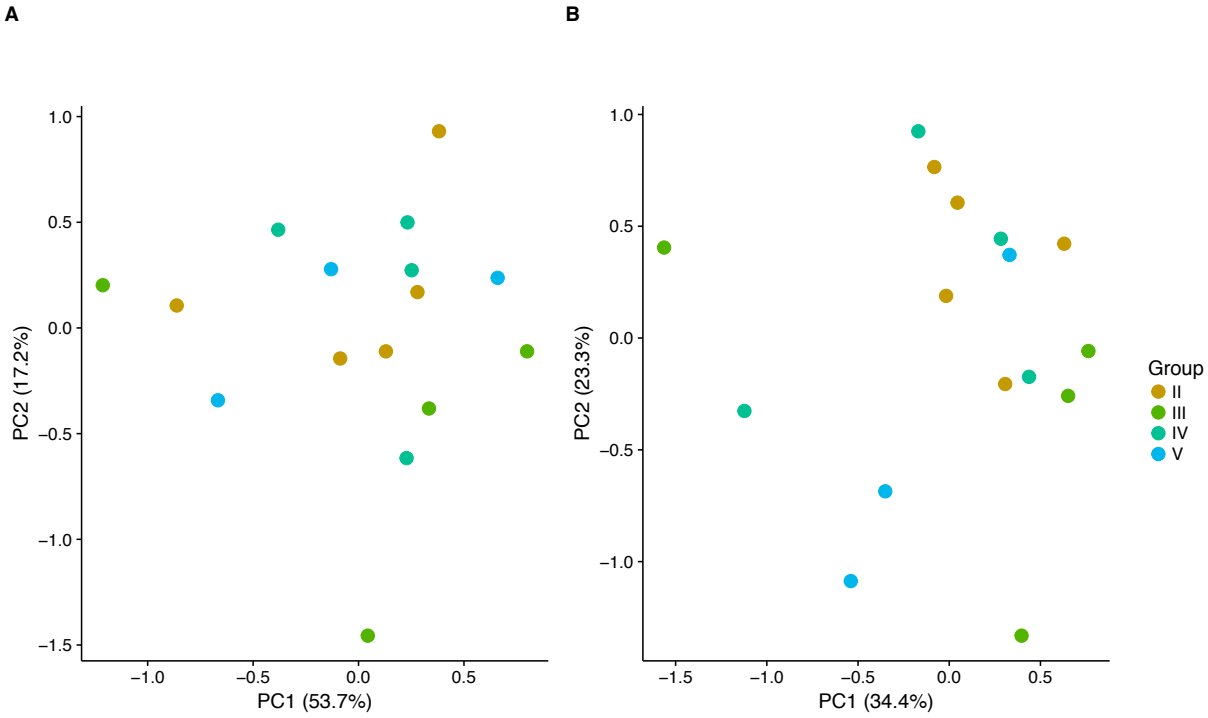

Figure S12

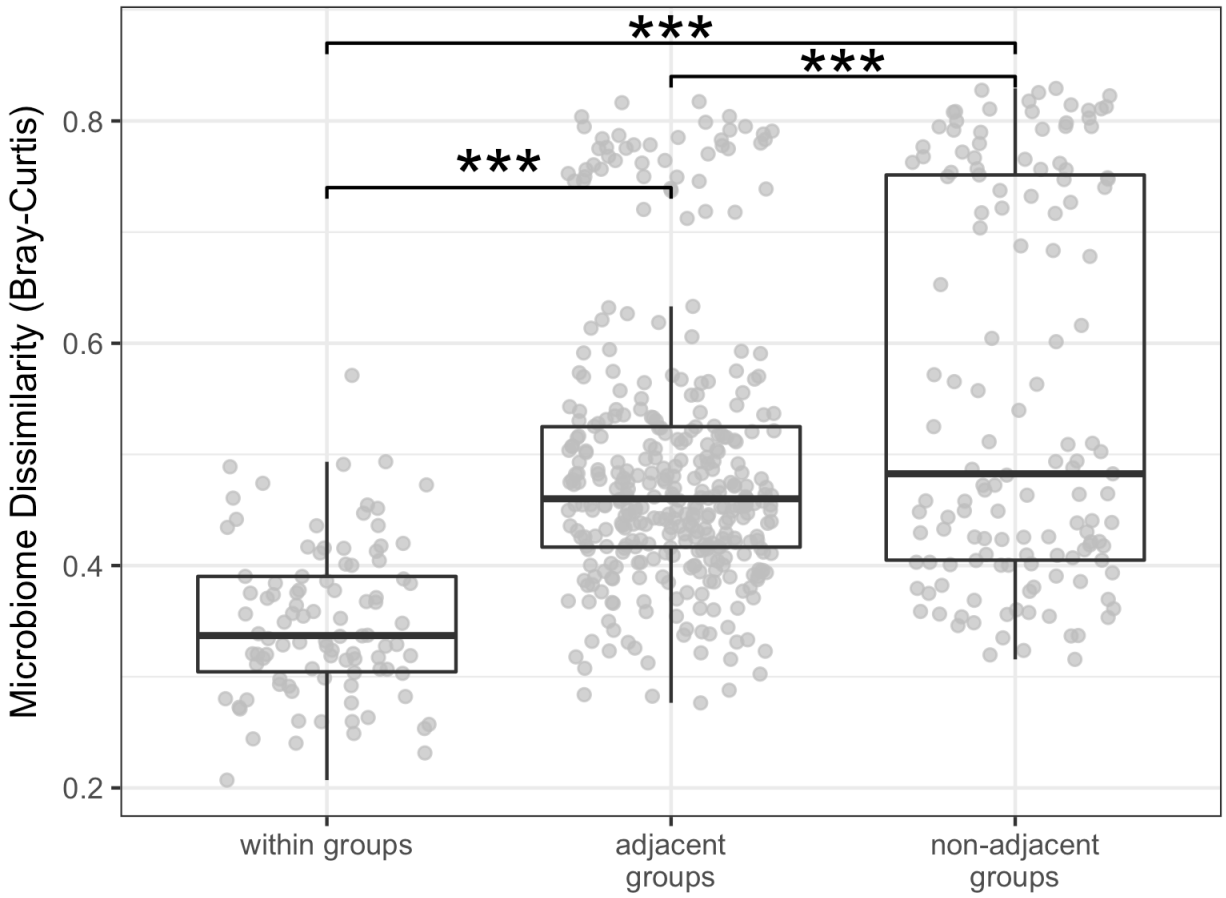
***
***
***
Microbiome Dissimilarity (Bray-Curtis)
0.8
0.6
0.4
0.2
within groups
adjacent groups
non-adjacent groups

403 **Figure S13**

404

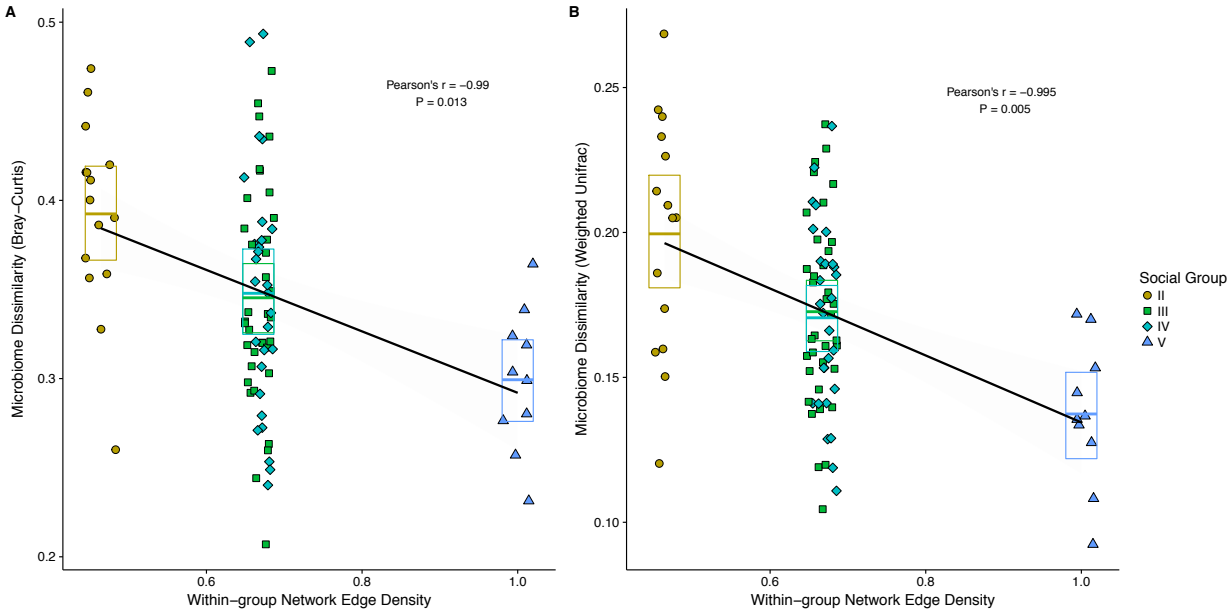

405

406

Figure S14

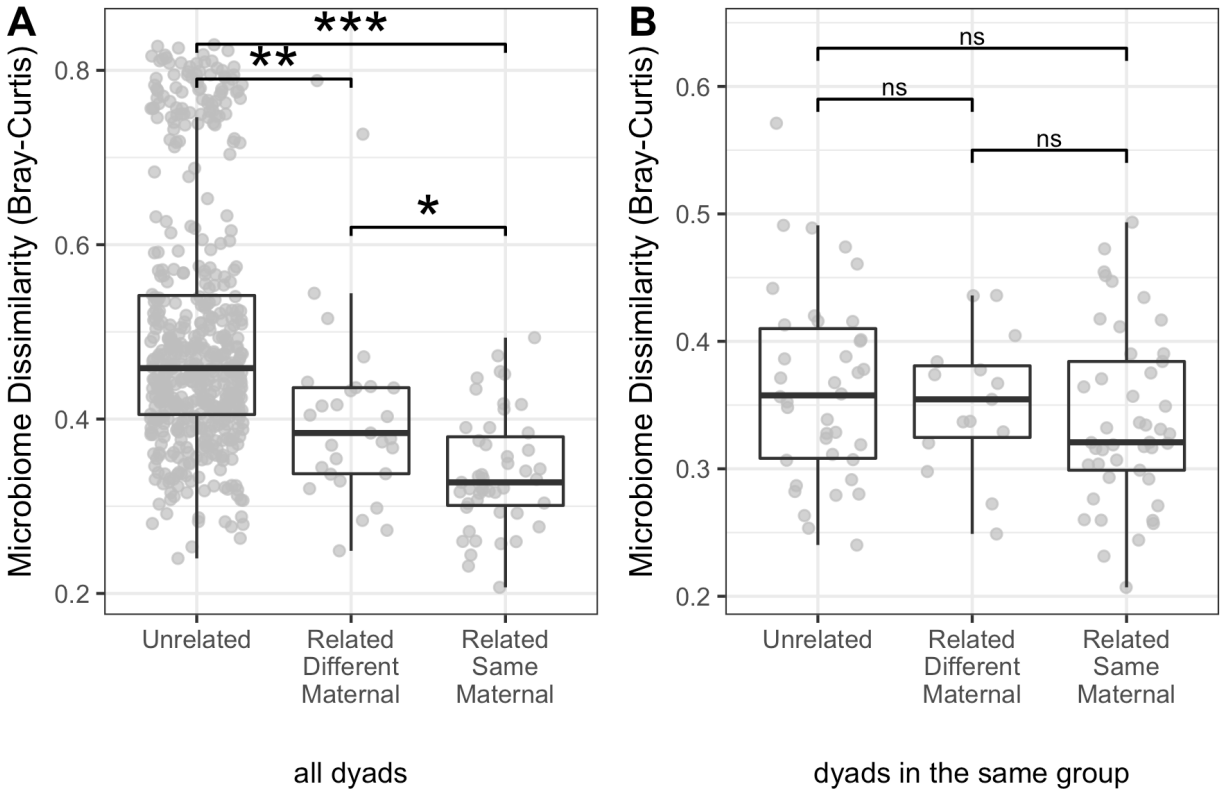
A
B
Microbiome Dissimilarity (Bray-Curtis)
0.8
0.6
0.4
0.2
***
**
*
ns
ns
ns
Unrelated
Related Different Maternal
Related Same Maternal
all dyads
dyads in the same group

Figure S15

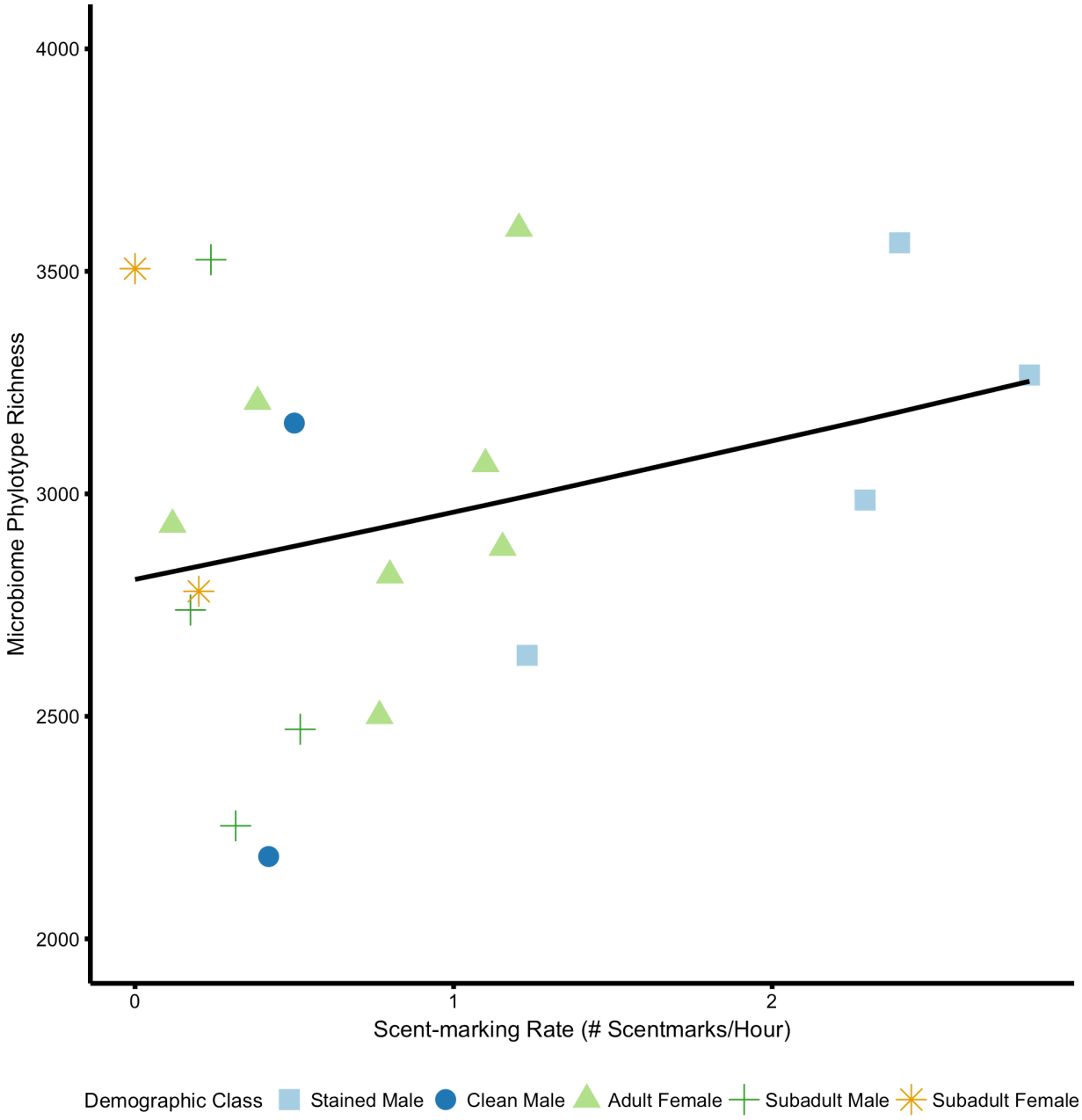
4000
3500
3000
2500
2000
Microbiome Phylotype Richness
0
1
2
Scent-marking Rate (# Scentmarks/Hour)
Demographic Class
Stained Male
Clean Male
Adult Female
Subadult Male
Subadult Female

Figure S16

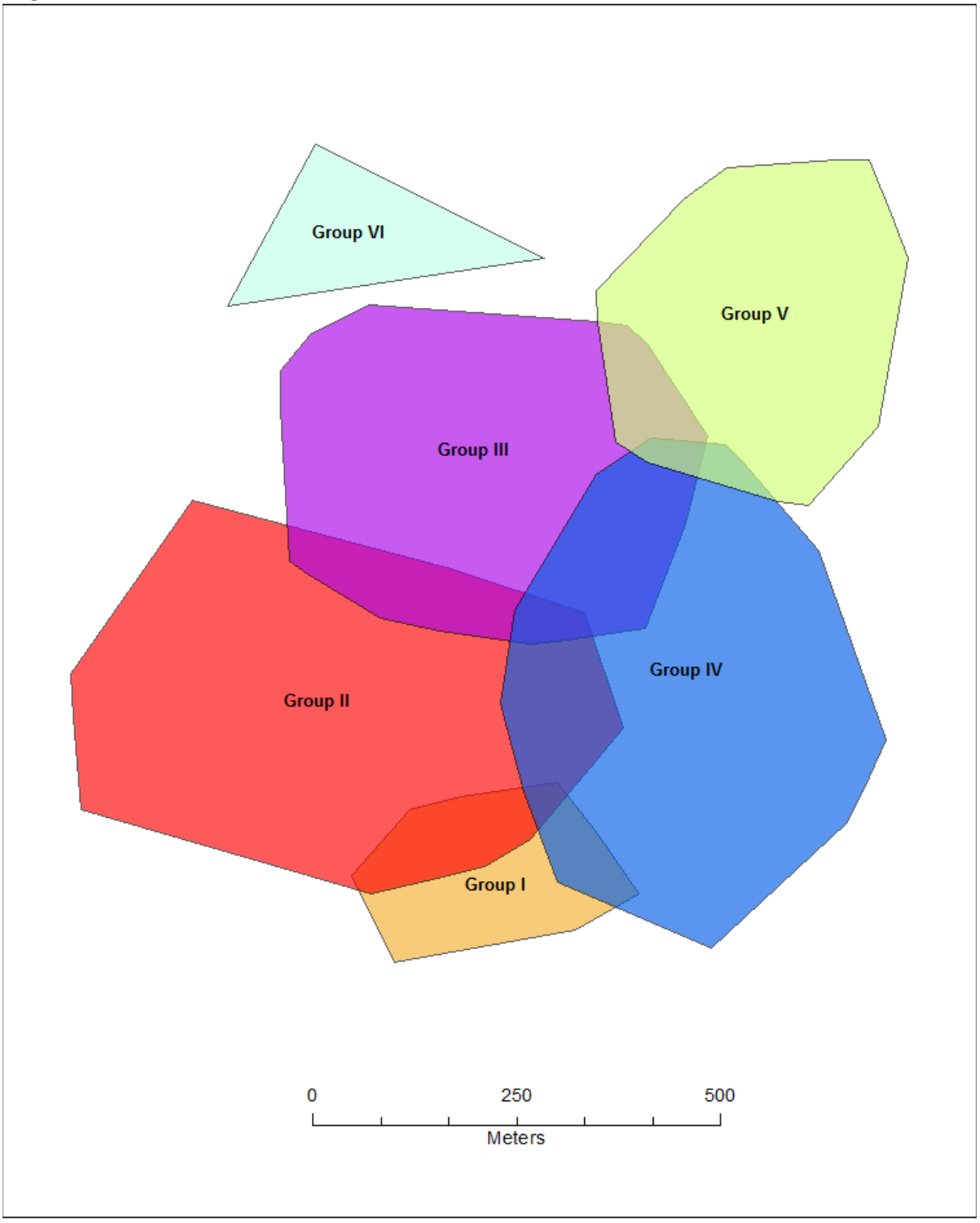
Group VI
Group V
Group III
Group IV
Group II
Group I
0
250
500
Meters

Table S1. Sample names and corresponding metadata. Summary of data available for Verreaux's sifaka social groups and individuals sampled in this study. Data abbreviations: genetic data (G), social behavior (SB), feeding behavior (FB), scent-marking behavior (SM), adult (A), subadult (S), juvenile (J). Recently dispersed males are bolded. Data were collected at Ankoatsifaka Research Station in Kirindy Mitea National Park.

Group	ID	Data	Sex	Age	Dominance/ Male chest status	Date	Latitude	Longitude
Camp	Camp 1					6/21/12	-20.795108	44.164616
	Camp 2					7/28/12	-20.795108	44.164616
	Camp 3					7/28/12	-20.795108	44.164616
	Camp 4					6/25/12	-20.795108	44.164616
	Camp 5					6/29/12	-20.795108	44.164616
	Camp 6					6/29/12	-20.795108	44.164616
I	I-F1	G	F	A		7/10/12	-20.787902	44.174563
	I-F2	G	F	A		7/17/12	-20.787506	44.174798
	I-M1	G, SB	M	A	Clean	6/20/12	Capture	Capture
	I-M2	G	M	A	Stained	7/17/12	-20.787655	44.174655
II	**II-M1**	G, SB, FB, SM	M	A	Subordinate/ Clean	7/23/12	-20.785467	44.172351
	II-M2	G, SB, FB	M	A	Subordinate/ Clean	7/23/12	-20.785467	44.172351
	II-M3	G, SB, FB, SM	M	A	Dominant/ Stained	7/15/12	-20.784029	44.172631
	II-F1	G, SB, FB, SM	F	A	Dominant	7/23/12	-20.785467	44.172351
	II-F2	G, SB	F	J		7/15/12	-20.784096	44.172153
	II-F3	G, SB, FB, SM	F	A	Subordinate	7/23/12	-20.785467	44.172351
III	III-M1	G, SB, FB, SM	M	A	Dominant/ Stained	6/24/12	Capture	Capture
	III-M2	G, SB, SM	M	S		7/24/12	-20.782915	44.175407
	III-M3	G, SB, FB, SM	M	A	Subordinate/ Clean	7/16/12	-20.782915	44.175407
	III-M4	G, SB, SM	M	S		7/3/12	-20.782366	44.172035
	III-F1	G, SB	F	J		7/24/12	-20.783205	44.175449
	III-F2	G, SB	F	J		7/3/12	-20.782383	44.171556
	III-F3	G, SB, FB, SM	F	A	Subordinate	7/24/12	-20.783196	44.175182
	III-F4	G, SB	F	J		7/24/12	-20.783196	44.175182
	III-F5	G, SB, FB, SM	F	A	Dominant	7/24/12	-20.783205	44.175449
IV	**IV-M1**	G, SB, FB, SM	M	S		7/25/12	-20.787493	44.176167
	IV-M2	G, SB, FB, SM	M	A	Stained	7/9/12	-20.784714	44.175641
	IV-M3	G, SB	M	J		7/9/12	-20.78516	44.175529
	IV-M4	G, SB	M	J		7/25/12	-20.787493	44.176167
	IV-F1	G, SB	F	J		7/9/12	-20.78516	44.175529
	IV-F2	G, SB, SM	F	S		7/25/12	-20.787493	44.176167
	IV-F3	G, SB, FB, SM	F	A	Dominant	7/25/12	-20.787726	44.176175
	IV-F4	G, SB, FB, SM	F	A	Subordinate	7/9/12	-20.78516	44.175529
V	V-F1	G, SB, FB, SM	F	A		7/19/12	-20.780978	44.177685
	V-F2	G, SB, SM	F	S		7/4/12	-20.781778	44.175369
	V-F3	G, SB	F	J		7/4/12	-20.781975	44.17582
	V-M1	G, SB, FB, SM	M	S		7/26/12	-20.783204	44.177087
	V-M2	G, SB, FB, SM	M	A	Stained	7/4/12	-20.781778	44.175369
VI	VI-F1	G	F	A		7/2/12	-20.781799	44.172333
	VI-F2	G	F	A		7/20/12	-20.780155	44.174486
	VI-M1	G	M	A	Stained	7/28/12	-20.779402	44.171545
	VI-U1					7/11/12	-20.77981	44.170482
	VI-U2					7/20/12	-20.779524	44.17233
	VI-U3					7/28/12	-20.779432	44.171258
	VI-U4					7/11/12	-20.779537	44.170558
	VI-U5					7/28/12	-20.77959	44.171239
	VI-U6					7/28/12	-20.779528	44.171666
Total N	47							

Table S2. Socially structured bacterial phyla, families, and genera among seven social groups of Verreaux's sifaka in Kirindy Mitea National Park. For each significant bacterial taxon, the ranking score, the contrast in each social group (the standardized mean difference between the phylum's abundance in that group versus its overall mean abundance), and the FDR-adjusted *P* value are shown. The microbial taxa that distinguished members of Groups I-V were Fibrobacteraceae (Fibrobacteres), Order Burkholderiales, *Flexispira,* Enterobacteriaceae, *Escherichia*, Desulfovibrionaceae (Proteobacteria), *Parabacteroides* (Bacteroidetes), Order Clostridiales (Firmicutes), and Order RF39 (Tenericutes). Sifaka in Groups VI and Camp showed higher abundance of taxa related to Actinobacteria (*Collinsella, Coriobacterium, Corynebacterium, Aldercreutzia*) and Firmicutes (*Coprobacillus*, Lachnospiraceae, Planococcaceae, unclassified Clostridiales). Groups IV and V were enriched in *Campylobacter* (Proteobacteria) and Cyanobacteria, whereas Groups I, II, and III were enriched in [Paraprevotellaceae] (Bacteroidetes), Bacillaceae (Firmicutes), and [Cerasicoccaceae] (Verrucomicrobia).

Phylum	Score	I	II	III	IV	V	VI	Camp	*P*
Bacteroidetes	33.109	-1.975	3.527	1.224	-3.945	-1.316	0.457	1.801	0.000
Firmicutes	30.716	-0.061	-2.682	-3.203	-0.123	-0.151	3.323	2.869	0.000
Synergistetes	26.789	1.732	1.712	-0.506	2.055	1.699	-2.751	-3.204	0.000
Unclassified	25.339	1.867	-3.405	-1.093	3.471	0.053	0.207	-1.07	0.000
Actinobacteria	22.976	-0.966	-0.907	-2.284	-1.295	-0.527	2.493	3.415	0.000
Verrucomicrobia	22.353	1.652	-1.484	1.18	1.592	2.286	-2.104	-2.713	0.000
Proteobacteria	14.024	0.93	-0.314	1.209	0.012	2.52	-2.023	-1.845	0.000
Cyanobacteria	13.827	-0.356	-1.55	-1.131	1.869	2.634	-0.061	-1.287	0.000
Fusobacteria	9.122	-0.777	-0.5	-0.529	-1.231	0.018	1.512	1.361	0.033
Fibrobacteres	8.872	0.304	-0.015	1.169	-2.282	-0.458	-0.394	1.841	0.033
Family	**Score**	**I**	**II**	**III**	**IV**	**V**	**VI**	**Camp**	***P***
Firmicutes									
Lactobacillales-Aerococcaceae	40.355	0.853	3.756	2.904	-3.686	-3.132	-0.087	-0.746	0.000
Bacillales-Staphylococcaceae	34.657	1.499	0.611	-2.262	2.813	3.348	-3.523	-1.305	0.000
Lactobacillales-Streptococcaceae	31.881	0.767	-1.114	1.417	3.148	2.15	-2.949	-3.253	0.000
Clostridiales-Lachnospiraceae	31.409	-0.272	-2.692	-0.881	-1.099	-2.275	4	2.584	0.000
Unclassified Lactobacillales	31.074	1.389	0.617	1.168	3.016	0.983	-3.728	-3.064	0.000
Lactobacillales-Enterococcaceae	29.375	-1.404	-1.777	-1.569	-0.178	-2.295	3.977	2.434	0.000
Clostridiales-Eubacteriaceae	25.754	-0.1	1.218	3.904	-1.952	-0.684	-3.136	0.79	0.000
Unclassified Bacillales	22.929	2.381	0.462	3.001	-0.729	-1.702	-2.885	-0.196	0.000
Clostridiales-Peptostreptococcaceae	18.846	-0.032	1.485	0.206	3.21	-0.826	-2.548	-1.549	0.000
Turicibacterales-Turicibacteraceae	16.862	1.445	2.874	0.026	-1.314	-0.912	0.243	-2.077	0.000
Clostridiales-Ruminococcaceae	15.63	-0.334	-1.584	1.809	2.252	0.585	-0.645	-2.586	0.000
Unclassified Coriobacteriales	14.814	-0.02	0.493	-0.878	3.088	0.388	-0.631	-2.533	0.000
Coriobacteriales-Coriobacteriaceae	14.512	-0.107	1.048	-0.206	1.196	2.275	-2.826	-0.832	0.000
Clostridiales-Veillonellaceae	10.379	1.95	0.058	1.438	0.417	-0.503	-2.073	-0.944	0.006
Clostridiales-Clostridiaceae	9.21	0.339	-0.786	1.891	0.878	-0.193	-0.135	-2.378	0.009
Unclassifed Clostridiales	9.198	0.089	-1.301	-1.89	1.372	0.393	1.841	-0.624	0.009
Erysipelotrichales-[Coprobacillaceae]	8.029	-0.234	0.16	1.12	1.481	-0.753	-2.028	0.134	0.016
Proteobacteria									

Unclassified Rhizobiales	28.4	1.339	0.45	0.938	1.231	2.929	-3.326	-2.847	0.000
Desulfovibrionales-Desulfovibrionaceae	24.97	1.011	0.646	2.113	0.799	1.989	-3.213	-2.932	0.000
Rhodospirillales-Acetobacteraceae	22.016	1.533	-0.395	2.859	0.665	0.695	-2.743	-2.415	0.000
Vibrionales-Vibrionaceae	20.433	0.921	0.776	1.698	0.876	1.648	-3.327	-2.134	0.000
Burkholderiales-Comamonadaceae	18.184	1.724	0.862	2.176	-0.123	0.465	-2.356	-2.382	0.000
Enterobacteriales-Enterobacteriaceae	17.879	0.533	1.996	0.58	-3.143	-1.177	-0.454	2.038	0.000
Rhizobiales-Methylobacteriaceae	17.571	1.461	1.125	2.357	-0.892	0.44	-1.974	-2.2	0.000
[Entotheonellales]-[Entotheonellaceae]	15.614	0.669	0.405	0.236	2.572	0.49	-1.703	-2.584	0.000
Pseudomonadales-Moraxellaceae	15.47	1.319	2.615	-0.92	0.442	-2.569	-0.603	-0.046	0.000
Pseudomonadales-Pseudomonadaceae	14.336	0.781	1.669	0.192	1.713	0.037	-3.025	-0.944	0.000
Rhizobiales-Hyphomicrobiaceae	14.093	-0.902	-0.674	-1.389	-0.683	-1.067	3.01	1.271	0.000
Aeromonadales-Succinivibrionaceae	10.35	0.219	0.314	0.098	0.341	1.732	-2.729	0.621	0.006
Burkholderiales-Oxalobacteraceae	10.147	0.992	1.953	0.243	0.668	-0.7	-1.604	-1.282	0.006
Campylobacterales-Campylobacteraceae	5.748	0.283	0.732	0.732	0.745	-0.622	-1.631	-0.173	0.038
Actinobacteria									
Rubrobacterales-Rubrobacteraceae	27.615	0.103	2.032	0.205	2.645	1.418	-3.542	-2.472	0.000
Solirubrobacterales-Unclassified	21.808	-0.135	0.021	-1.351	-3.01	-0.558	2.266	2.919	0.000
Actinomycetales-Mycobacteriaceae	21.216	-0.24	1.106	2.671	-0.116	1.631	-2.463	-2.527	0.000
Actinomycetales-Geodermatophilaceae	18.889	0.963	-0.963	0.705	2.201	1.612	-1.464	-2.917	0.000
Solirubrobacterales-Solirubrobacteraceae	16.364	1.202	1.206	-0.111	2.618	-0.905	-2.219	-1.576	0.000
Actinomycetales-Actinomycetaceae	11.826	0.982	1.092	-0.049	0.774	1.324	-1.382	-2.322	0.002
Actinomycetales-Microbacteriaceae	8.931	0.335	-1.491	1.426	1.447	0.249	-0.716	-1.487	0.011
Actinomycetales-Pseudonocardiaceae	8.522	-0.284	1.427	1.094	-1.342	-0.695	0.828	-1.304	0.012
Actinomycetales-Corynebacteriaceae	6.721	1.132	0.739	0.112	-1.101	-1.506	-0.08	0.908	0.027
Bacteroidetes									
Bacteroidales-Porphyromonadaceae	24.617	1.124	1.416	2.009	0.521	1.478	-3.398	-2.67	0.000
Bacteroidales-Bacteroidaceae	16.931	1.334	0.448	0.623	0.58	2.211	-2.068	-2.556	0.000
Bacteroidales-Prevotellaceae	13.557	2.496	0.903	-0.952	1.347	-0.205	-1.194	-1.787	0.000
Bacteroidales-[Paraprevotellaceae]	10.195	0.386	-0.324	0.464	2.097	0.522	-1.048	-2.154	0.006
Verrucomicrobia									
[Cerasicoccales]-[Cerasicoccaceae]	21.996	-1.11	0.079	1.85	2.45	1.445	-2.638	-2.315	0.000
Cyanobacteria									
Unclassified YS2	21.575	-0.699	-2.251	-0.783	-0.642	-1.662	3.404	2.004	0.000
Synergistetes									
Synergistales-Dethiosulfovibrionaceae	20.811	0.557	-1.368	-1.256	-2.34	-0.574	2.016	3.173	0.000
Tenericutes									

Unclassified RF39	18.453	1.47	-0.412	1.548	1.63	0.997	-2.018	-3.02	0.000
Genus	**Score**	**I**	**II**	**III**	**IV**	**V**	**VI**	**Camp**	***P***
Atopobium	36.459	2.114	-2.172	4.397	-2.71	-2.506	-0.167	0.784	0.000
Parabacteroides	33.294	1.959	3.11	1.052	0.432	1.033	-3.757	-3.001	0.000
Collinsella	32.754	0.266	0.853	-2.189	-1.827	-3.34	3.336	2.715	0.000
Coprobacillus	31.489	0.73	-1.314	-2.208	-0.819	-2.853	2.703	3.678	0.000
Blautia	30.828	1.565	-2.531	0.466	-2.996	-1.656	1.86	3.384	0.000
Coriobacterium	30.089	-0.214	0.963	-2.207	-1.769	-2.923	3.095	2.861	0.000
[Prevotella]	30.019	1.322	0.839	-3.107	1.855	3.236	-3.071	0.26	0.000
Adlercreutzia	29.592	1.395	-2.432	-0.016	-2.662	-1.999	2.991	2.603	0.000
Bacteroides	27.876	-0.303	1.666	2.234	-3.359	-1.551	-1.553	3	0.000
Moryella	27.615	0.625	-0.44	2.269	2.554	1.033	-4.121	-1.73	0.000
Anaerofustis	27.169	-0.27	-0.686	-2.266	-0.622	-2.626	3.365	2.744	0.000
Streptococcus	26.618	1.32	-1.751	-2.852	-1.771	-0.054	3.463	1.972	0.000
Prevotella	26.463	-0.255	3.798	1.457	-2.832	-2.265	0.638	-0.773	0.000
Phascolarctobacterium	24.2	2.274	2.182	0.968	0.477	0.125	-1.935	-3.596	0.000
Butyrivibrio	23.831	-1.445	-1.595	-3.404	2.307	0.14	2.105	1.606	0.000
Campylobacter	22.837	-0.272	0.95	0.403	1.893	2.746	-2.819	-2.542	0.000
YRC22	20.222	-0.744	-2.124	3.722	-1.14	-0.485	-1.225	1.535	0.000
Cloacibacillus	20.195	1.243	1.418	0.477	0.463	2.075	-1.843	-3.286	0.000
Corynebacterium	19.846	-0.873	-0.956	-1	-1.341	-1.427	2.031	3.3	0.000
Bacillus	19.085	-1.146	-0.997	-0.29	-0.905	-1.24	0.611	3.741	0.000
Oscillospira	19.006	1.679	2.562	0.424	-0.104	0.045	-0.876	-3.359	0.000
Flexispira	18.059	0.549	1.316	0.308	0.751	2.444	-3.037	-1.66	0.000
Pseudomonas	17.266	-1.169	-0.94	-1.367	-0.958	-0.795	2.161	2.796	0.000
Bilophila	16.626	1.434	2.639	1.252	-1.209	0.039	-1.573	-2.135	0.000
Coprococcus	16.316	-0.12	1.303	-1.554	-1.393	-1.428	3.132	-0.176	0.000
Sphingobium	16.01	-0.557	-1.171	-0.263	-0.747	-1.444	0.683	3.317	0.000
Roseburia	15.723	-1.791	1.304	-2.413	1.44	2.077	0.23	-0.773	0.000
Peptoniphilus	15.544	-0.893	-0.798	-0.771	-1.055	-1.469	2.403	2.166	0.000
Desulfovibrio	15.52	0.938	-0.146	0.317	1.539	1.216	-0.25	-3.574	0.000
Fibrobacter	15.338	0.395	1.836	1.711	-2.825	-1.17	-0.951	1.2	0.000
Escherichia	15.152	0.879	0.878	1.781	-0.055	1.497	-2.91	-1.603	0.000
Actinomycetospora	15.069	-0.839	-1.089	-0.99	-0.733	-0.839	1.498	2.793	0.000
Enterococcus	13.954	2.178	-0.207	-2.052	-0.881	-0.225	-0.215	2.259	0.000
Methylobacterium	12.357	-0.672	-0.771	-0.639	-0.372	-1.417	0.912	2.738	0.000
[Ruminococcus]	12.247	1.278	0.961	1.56	-2.001	-0.236	-1.985	0.943	0.000
Facklamia	12.104	-0.693	-0.772	-1.06	-0.892	-0.238	1.281	2.315	0.000
Oxalobacter	11.108	1.418	1.707	0.373	-1	1.243	-1.8	-1.233	0.000
Clostridium	11.044	-0.916	-1.21	-0.346	-0.996	-0.666	1.75	2.058	0.000
Ruminococcus	9.923	-0.315	0.826	-2.064	1.437	-0.681	-0.835	1.867	0.000
Staphylococcus	9.527	-0.487	-1.111	-0.647	-0.855	-0.263	1.53	1.683	0.000
Pseudonocardia	9.19	-0.782	-0.836	-0.274	-0.203	-0.44	0.149	2.272	0.000
Slackia	8.165	0.054	1.232	1.355	-0.815	-1.19	0.24	-1.141	0.000
Anaerostipes	8.053	0.483	0.713	0.475	0.991	0.5	-0.583	-2.568	0.000
Comamonas	7.755	-0.944	-1.05	-0.315	-0.402	0.293	1.378	0.768	0.000
Delftia	7.677	-0.279	-0.206	-0.015	-0.872	-0.66	0.318	1.674	0.000
Acinetobacter	7.571	-0.932	-0.413	0.006	-0.393	-0.929	0.576	1.806	0.000
J2-29	7.113	-0.398	-0.08	-0.769	-0.635	-0.35	1.215	0.926	0.000
Dermacoccus	6.942	-0.321	-0.148	-0.486	-0.21	-0.279	1.474	-0.255	0.000
Candidatus Nitrososphaera	6.893	-0.112	-0.24	-0.1	-0.228	-0.203	-0.333	1.289	0.000
Rubrobacter	6.802	-0.21	-0.338	-0.158	0.108	-0.208	-0.484	1.341	0.000

435 Abundances for each taxonomic level were determined to be significant using the nonparametric SAMseq
436 algorithm (FDR adjusted $P < 0.05$).

437

Table S3. Pairwise social and genetic predictors of weighted Unifrac distance among Verreaux's sifaka at Kirindy Mitea National Park. Posterior mean, 95% credible interval (95% CIs), and *P*-value based on Markov chain Monte Carlo sampling for fixed-effect parameters.

	Parameter	Mean	95% CI	*P*	Interpretation
Group membership N_{pairs} = 167 DIC: -594.57	Intercept	0.25	(0.23, 0.26)	**< 5 x 10^{-5}**	
	Same group	-0.06	(-0.08, -0.04)	**< 5 x 10^{-5}**	Pairs in the same social group have less dissimilar microbiota
	Related	0.005	(-0.01, 0.02)	0.6	No significant correlation
Social distance N_{pairs} = 167 DIC: -628.98	Intercept	0.18	(0.15, 0.2)	**< 5 x 10^{-5}**	
	Path length	9.07 x 10^{-6}	(6.19 x 10^{-6}, 1.2 x 10^{-5})	**< 5 x 10^{-5}**	Pairs that are farther apart in the social network have more dissimilar microbiota
	Related	8.11 x 10^{-4}	(-0.02, 0.01)	0.66	No significant correlation

Baseline relatedness (not related) is not shown. Individual identity within each pair was included as a random effect. Bolded relationships are significant at $P < 0.05$.

Table S4. Predictors of within-host gut microbiome richness for 29 Verreaux's sifaka inhabiting Kirindy Mitea National Park. The coefficient estimate, standard error, z value, and Pr(>|z|) value are shown for fixed effect parameters.

Parameter	Estimate	Std. Error	z value	Pr(>|z|)	Intreptation
Intercept	7.89	0.02	506.4	**< 2 x 10^{-16}**	
Weighted In Degree Centrality	4.66	1.22	3.8	**0.0001**	Individuals that frequently receive grooming have greater microbial diversity
Weighted Out Degree Centrality	18.62	1.75	10.6	**< 2 x 10^{-16}**	Individuals that frequently initiate grooming have greater microbial diversity

Group membership was included as a random effect. Bolded relationships are significant at $P < 0.05$.

Filename: Perofsky_2017_ProcB_ESM_2_Nov_6_2017.docx
Folder: /Users/amandaperofsky12/Library/Containers/com.microsoft.Word/Data/Documents
Template: /Users/amandaperofsky12/Library/Group Containers/UBF8T346G9.Office/User Content.localized/Templates.localized/Normal.dotm
Title:
Subject:
Author: Perofsky, Amanda C
Keywords:
Comments:
Creation Date: 11/6/17 7:06:00 PM
Change Number: 2
Last Saved On: 11/6/17 7:06:00 PM
Last Saved By: Perofsky, Amanda C
Total Editing Time: 0 Minutes
Last Printed On: 11/6/17 7:06:00 PM
As of Last Complete Printing
Number of Pages: 31
Number of Words: 6,002
Number of Characters: 97,315 (approx.)